RESEARCH ARTICLE OPEN ACCESS

Investigation of NO_2 Absorption Behaviour around 593 nm for Seeding Purposes

T. Sander*, P. Altenhöfer*, L. Kleiner*, Ch. Mundt*
**(Institute for Thermodynamics, Department of Aerospace Science, Bundeswehr University Munich, Germany)*
Corresponding Author : T. Sander

ABSTRACT
At the Institute for Thermodynamics at the Bundeswehr University Munich a piston-driven shock tunnel is operated to investigate structures of space transportation systems under reentry conditions. For temperature measurements in the nozzle reservoir under single-shot conditions, laser-induced grating spectroscopy (LIGS) was identified as best-suited measurement technique. However, under moderate conditions seeding of the test gas with NO_2 was used successfully to improve the signal-to-noise ratio of thermal signals. For a better understanding and an optimization of the seeding process, an optical setup for an absorption measurement in a test cell in the used spectral range of the LIGS measurements (592 nm - 596 nm) was developed. The measurements of NO/N_2-seeded dry air showed excellent agreement with reference data from literature for NO_2. Consequently, the formation process of NO_2 and the temporal evolution of the NO_2 concentration was investigated with the commercial Code Cosilab. The identification and validation of a suitable reaction mechanism was done by calculating concentrations in equilibrium condition and comparison to the NASA code CEA. The identified reaction mechanism was used to simulate the temporal development of NO_2 concentrations after filling the test cell with a NO/N_2-air mixture.
Keywords – absorption, shock tunnel, laser-optical measurements, reaction kinetics

---

Date Of Submission: 01-08-2019 Date Of Acceptance: 12-08-2019

I. INTRODUCTION

For the experimental simulation of the reentry of space transportation systems, the medium-sized piston-driven shock tunnel HELM (High Enthalpy Laboratory Munich) has been in operation at the Institute for Thermodynamics of the University of the Federal Armed Forces Munich since 2010 [1, 2]. For a better characterization of the flow conditions in the nozzle during experiments, knowledge of the temperature within the nozzle reservoir is highly desirable.

Optical measurement techniques are well suited for measurements in high-enthalpy flows as they do not influence the flow and are not subject to mechanical and thermal limits like probes. Further challenges for the measurement technique are the extremely high temperature and pressure as well as the very short measurement time in the nozzle reservoir of shock tunnels. Laser-induced grating spectroscopy (LIGS) with its variants laser-induced electrostrictive grating spectroscopy (LIEGS) and laser-induced thermal grating spectroscopy (LITGS) offers the possibility of precise temperature measurement in combination with a high temporal resolution having been chosen after a detailed analysis of potential optical measurement techniques [3]. Examples for versatile applications of laser-induced gratings can be found in literature [4-6]. The physical background of the formation of laser-induced electrostrictive and thermal gratings and their reading is described in detail in [7-10].

In own examinations a LIGS measurement setup was developed and realized [11] and its operability with electrostrictive gratings (LIEGS) and thermal gratings (LITGS) was proven first in a test cell [3] and later in a conventional shock tube [12, 13]. As measurements using thermal gratings are promising especially at high temperatures, expected within the HELM facility, LITGS is regarded as a promising technique for experiments under high-enthalpy conditions [14, 15]. For the formation of a thermal grating, the presence of an absorbing species in the test gas is essential. The absorbing species (e.g. NO_2) is either formed during experiments under high-enthalpy conditions or can be added before the experiment (seeding). Especially under moderate conditions, seeding may be necessary for obtaining a high signal-to-noise ratio. However, as pure NO_2 is a toxic and highly corrosive substance, it is unsuitable for seeding purposes. Therefore, the authors decided to mix a commercial $NO\text{-}N_2$ test gas with air, in order to generate a small, but sufficient concentration of the absorbing species NO_2.

For a better understanding and an optimization of this seeding process, initially in this

work absorption spectra of test gas mixtures consisting of NO, N_2 and air were recorded and compared with corresponding reference data from literature investigating the absorption of NO_2. A good agreement could be found. Then, a reaction mechanism was validated using the commercial tool Cosilab [16] with results of equilibrium calculations from the NASA code Chemical Equilibrium with Applications, CEA [17] for the numerical simulation of chemical reactions. Subsequently, calculations of temporal changes in concentrations in a virtual reactor were carried out using the validated mechanism. Additionally, a time-resolved absorption measurement for 45 minutes was performed in a test cell, which was filled with a seeded test gas mixture. The comparison of both data sets showed satisfactory agreement, albeit the measured concentration decreased after about 15 minutes, whereas the calculated remained constant.

II. MEASURING PRINCIPLE

Absorption spectroscopy is a well established analytical procedure in physics and chemistry. With this technique the spectral intensity distribution of electromagnetic radiation after interaction with atoms and molecules is detected. While infrared spectroscopy is mainly applied to gas analysis or determination of the chemical structure of a sample, the spectroscopy in the visible and ultraviolet range is used for the concentration measurements of atoms, ions and species. The Beer-Lambert law describes the strength and dependance of wavelength of the absorption of electromagnetic waves for a homogeneous isotropic substance. The absorbance A, which characterizes the wavelength-dependent attenuation of the light, can be described with (1):

$$A = log\left(\frac{I_0}{I}\right) = \varepsilon(\lambda)\, c_i\, x \qquad (1)$$

where I_0 is the intensity of a monochromatic beam, I the intensity of this beam after passing the substance, $\varepsilon(\lambda)$ the spectral extinction coefficient, c_i the concentration of the absorbing substance and x the length of the light path through the absorbing medium.

III. EXPERIMENTAL SETUP

The experimental setup is shown in Fig. 1. The laser beam was generated by a system consisting of a Nd:YAG laser (wavelength, 532 nm; maximum pulse energy, 400 mJ; pulse duration, 20 ns) and a dye laser (dye, Rhodamine B; efficiency ≈ 28%, linewidth 0.15 cm^{-1}). The ratio between the pulse energy on sensor 1 (Coherent J-10MB-HE) and sensor 2 (Coherent J-25MT-10KHZ) resulting from the optical properties of the beam splitter was measured before the absorption measurements. A third energy sensor (Coherent J-10MB-LE) was placed inside the dye laser to measure the relative pulse energy of the Nd:YAG laser beam and to record its energy fluctuation. Using a mirror system, the beam passed through the test cell three times, whereby the effective path length could be increased from 200 mm to 600 mm. The third mirror, which deflected the laser beam into the test cell, caused stray light due to imperfect reflection of the laser beam. This reflection could be detected by a spectrograph (Solar TII MS3504i) and an ICCD detector (Princeton Instruments PI-MAX2) and was used to monitor the wavelength of the laser beam.

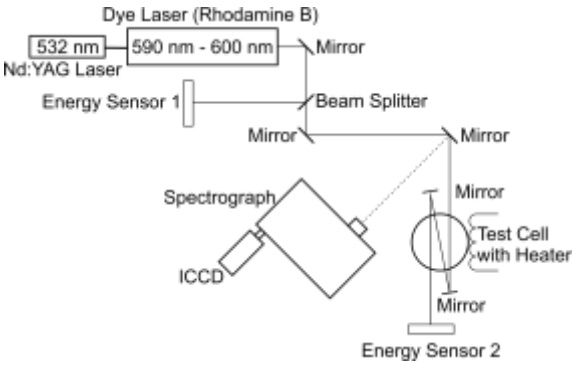

Fig. 1: Schematic of the setup for the absorption measurements

The spectral detection system was calibrated with a neon lamp by using its emission lines in the range of the spectral range of the absorption measurements. It was found that the offset between the wavelength set in the control software of the dye laser and the wavelength measured with the spectrograph is approximately 0.037 nm (i.e. when the dye laser was adjusted to a wavelength of 593 nm, it delivered an emission at 592.963 nm). This accuracy was taken into account for the analysis of the experimental data.

The stainless steel test cell has an inner diameter of 100 mm and optical access via silica windows (Fig. 2). The transmission coefficient of the windows is higher than 0.9 in the spectral range from 260 nm to 1200 nm. The cell is capable of temperatures up to 70 °C and pressures up to 2 MPa. Heating can be carried out with a temperature-controlled heating pad. The cover plate offers access for gas supply as well as for a Pt100 resistance thermometer and a pressure gauge.

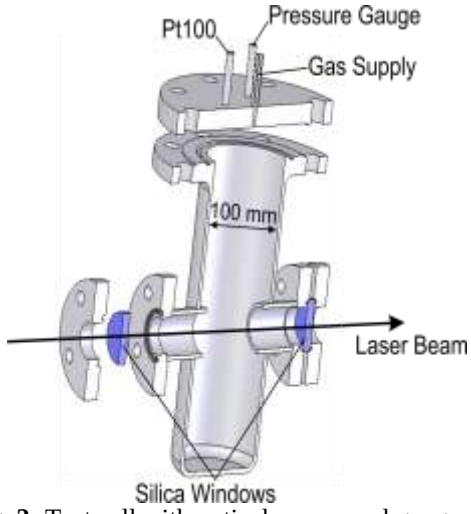

Fig. 2: Test cell with optical access and gauges for temperature and pressure

III.1 Absorption Spectrum of NO_2

The absorption system of one single electronic transition of NO_2 extends from the ultraviolet spectrum ($B^2B_2 - X^2A_1$) to the visible ($A^2B_1 - X^2A_1$) with a global maximum at 435 nm [18, 19]. Reference measurements of the whole spectrum as well as the range analyzed in this work are shown in Fig. 3. It can be seen that the absorption cross section around the maximum is approximately one order of magnitude higher than in the range from 592 nm to 596 nm investigated here. Furthermore, the magnified view shows that the measurement presented in [20] has the highest spectral resolution (0.0055 nm), while the other measurements have lower resolutions (resolution of [21]: 0.025 nm, resolution of [22]: 0.126 nm).

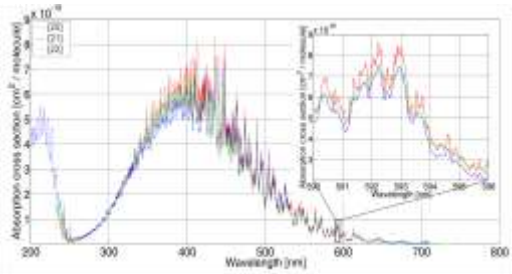

Fig. 3: NO_2 absorption cross sections of the utilized spectral reference data [20-22].

III.2 Data Processing

In order to derive data from the test cell measurements that could be compared to literature, the measured intensities require processing. Firstly, the measured intensities (reference laser energy measured with energy sensor 1, I_1, and measurement laser energy measured with sensor 2, I_2, see Fig. 1), were averaged over the number of laser pulses per wavelength increment. Secondly, the quotient of the averaged intensities I_1/I_2 was calculated, logarithmized and normalized by the first value of each data set. Additionally, the reference was normalized by the first value of the regarded spectrum. In this way, errors that might have arisen from the calculation of absolute values for absorption coefficients and absorption cross sections were prevented. For the concentration measurements at a single wavelength, the quotient of the intensities was calculated and normalized by the first measured value.

IV. RESULTS AND DISCUSSION

The measurements presented in this section were carried out with an initial NO concentration of 1320 ppm (mixture 1). In Fig. 4 the comparison of two measurements with reference data [20, 21] is shown. The temperatures in the test cell were 293 K and 353 K for measurement 1 and measurement 2, respectively. Both measurements were carried out at a pressure of 1 MPa and a spectral range from 592 nm to 596 nm with a wavelength increment $\Delta\lambda$ of 0.01 nm. For each measured value 50 laser pulses were accumulated.

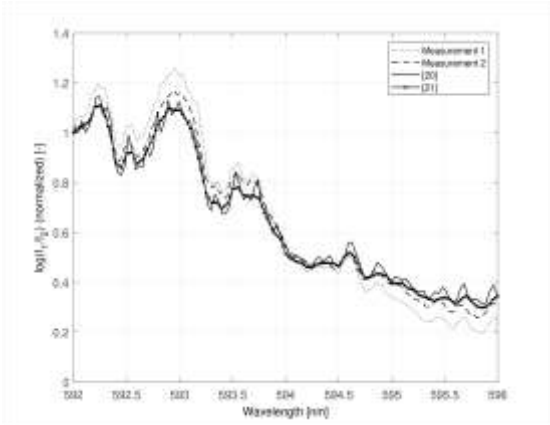

Fig. 4: Comparison of two absorption measurements (mixture 1, initial NO concentration 1320 ppm, p = 1 MPa, wavelength increment $\Delta\lambda$ = 0.01 nm, 50 laser pulses per increment) with reference data [20, 21]

It can be seen that the spectral features of the measurement data and the references are in good agreement in the regarded range. The maximum difference between the logarithmized intensity ratio at 595.8 nm is approximately 20% (reference [20] and measurement 2), whereas this difference is about 9% at 592.9 nm. The standard deviation of the energy measured inside the dye laser and with sensor 1 is between 7.6% (measurement 2) and 9% (measurement 1) with regard to the respective mean value. The spectral features of both measurements coincide better with reference [20] than the references [20] and [21] with each other. In the spectral range above 594.5 nm the difference between measurement 1 and the references becomes

larger, which may be a result of the observed increased standard deviation of the laser pulse energy compared to measurement 2. It is important to note that the aim of this measurement was not to measure absorption spectra of NO_2 with high precision but to prove the formation of the absorbing species NO_2 after filling the test cell with a mixture of NO, N_2 and air. For this purpose the obtained accuracy is regarded as sufficient.

In the next step, the spectral range from 592 nm to 594 nm was analyzed with the smallest wavelength increment possible with the current experimental setup ($\Delta\lambda$ = 0.001 nm). Comparison of this measurement with reference data [20, 21] is shown in Fig. 5.

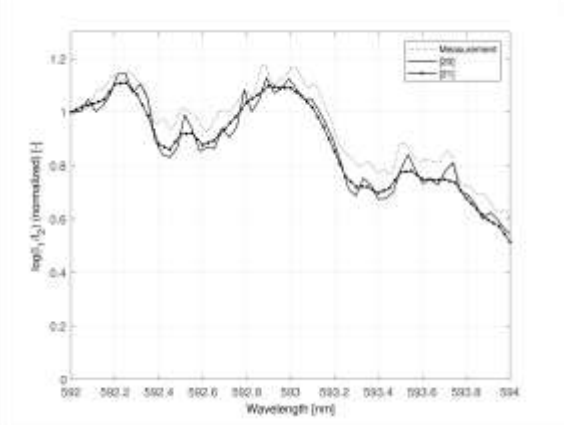

Fig. 5: Comparison of measurement (mixture 1, initial NO concentration 1320 ppm, p = 1 MPa, wavelength increment $\Delta\lambda$ = 0.001 nm, 50 laser pulses per increment) with reference data [20, 21]

Very good agreement of the data is observed, especially with reference [20]. The maximum difference between the logarithmized intensity ratios of the measurement with the references is approximately 17% at 593.3 nm. Again, the agreement between the spectral features of the measurement and reference [20] is better than the coincidence between the spectral features of reference [21] and reference [20], which can be explained by the higher spectral resolution of reference [20].

It can be stated that the presented measurements were carried out with low NO_2 concentrations and in a spectral range, where the absorption of NO_2 is comparatively weak (Fig. 3). The reference spectra [20-22] were measured partially with pure NO_2 and with a significantly higher optical path length through the absorbing medium (in one case several meters). Using the presented straightforward absorption measurement setup, a good agreement with the reference data could be found, which proves the NO_2 formation after filling the test cell with the gas mixture.

V. REACTION KINETICS

To optimize the seeding process, knowledge of the chemical processes taking place in the shock tube after filling is necessary. The calculations of reaction kinetics were performed with Cosilab. For the prediction of the temporal behavior of the species concentration, a homogeneous reactor with constant volume was filled with a NO-air mixture. As the formation of NO_2 occurs in several elementary reactions rather than in one global reaction, a reaction mechanism was required, which is capable of calculating the complete reaction kinetics. A literature review found four mechanisms describing the formation of NO_2 [23-26]. However, these mechanisms were developed for the description of complex combustion processes or atmospheric reactions, where among other species NO, air components, NO_2 and further nitrogen oxides are formed. On one hand a suitable mechanism had to reproduce equilibrium concentrations that were calculated with CEA, and on the other hand it had to simulate the temporal NO_2 concentration after filling the test cell. All described mechanisms were analyzed and compared and the mechanism of Volkov et. al. [23] showed the best accordance between measurement data and calculations. This mechanism is a sub-mechanism of nitrogen oxide formation kinetics during combustion and consists of 29 elementary reactions and 11 different species. It includes data from [26] and [27], which are given with a $\Delta\log k$ of ± 0.06 and ± 0.3, respectively, for the essential reactions.

V.1 Validation of the reaction mechanism on the basis of equilibrium state

The validation of equilibrium state was carried out by comparison with calculations performed using CEA. Investigations showed that NO and NO_2 reactions are dominated by the equilibrium between NO_2 and N_2O_4. Fig. 6 shows the comparison of the N_2O_4 mole fractions as a function of temperature at pressures of 0.1 MPa and 1 MPa.

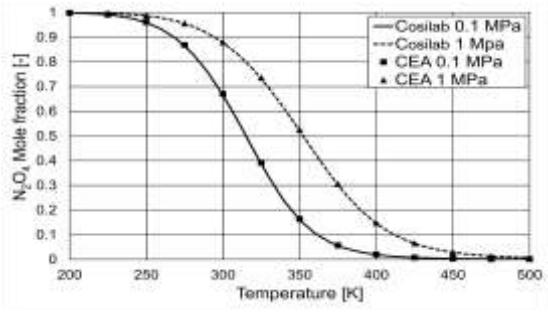

Fig. 6: Comparison of the N_2O_4 equilibrium concentration depending on temperature at pressures of 0.1 MPa and 1 MPa

The initial concentration of NO_2 was 100%. It can be seen that the concentration of N_2O_4 decreases with increasing temperature and decreasing pressure, and a good agreement between Cosilab calculations and CEA calculations is apparent.

When NO is added to air, a mixture of NO, NO_2, N_2O_3 and N_2O_4 will be formed by chemical reactions. The NO_2 concentration is determined by the temperature dependent equilibrium between NO_2 and N_2O_4. To analyze these equilibrium concentrations with the chosen mechanism, the test cell was filled with an initial concentration ratio of two parts NO to one part O_2. The results of the calculation with CEA and Cosilab at a pressure of 1 MPa are presented in Fig. 7. A good agreement between the CEA and Cosilab calculations can be seen again. It should be noted that the concentration of N_2O_3 is very small compared to the prevailing equilibrium between NO_2 and N_2O_4 in the analyzed temperature range from 295 K to 353 K. Only above 400 K a small concentration of NO is formed.

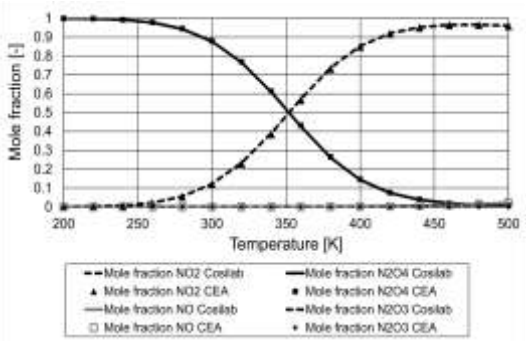

Fig. 7: Comparison of the equilibrium concentrations of NO, NO_2, N_2O_3 and N_2O_4 depending on temperature at a pressure of 1 MPa

V.2 Validation of the reaction mechanism on the basis of temporal changes in concentration

For a prediction of the NO_2 formation over time with Cosilab, the virtual test cell was filled with air (mole fraction N_2, 0.79, mole fraction O_2, 0.21) to a pressure of 0.1 MPa. After that, the cell was filled with a NO-N_2 mixture (1650 ppm NO diluted with N_2) to a total pressure of 1 MPa, which corresponds to an initial mixture given in Table 1 (mixture 2).

Table 1: Initial condition for the calculation of the reaction in the test cell

Species	N2	NO	O2
Mole fraction [%]	97.7515	0.1485	2.1

To evaluate the Cosilab calculations, two absorption measurements of the laser beam in the test cell were carried out for 45 minutes (measurement 1) and 35 minutes (measurement 2). The comparison of the data sets is given in Fig. 8.

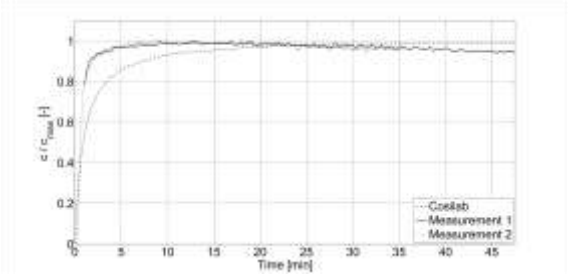

Fig. 8: Comparison of the temporal NO_2 concentration evolution calculated with Cosilab and measured by absorption (mixture 2, initial NO concentration 1485 ppm, p = 1 MPa, λ = 593 nm)

The concentration calculated with Cosilab was normalized by its maximum value after 60 minutes. For the determination of the experimental concentration gradients, the common logarithm of the intensity ratio of energy sensor 1 and energy sensor 2 (see Fig. 1) was calculated according to (1). The standard deviation of the energy measured with sensor 1 is 7.3% with regard to the respective mean value. The data then were smoothed by a Savitzky-Golay-filter [28] and normalized by the respective maximum concentration c_{max} of each measurement. Measurement 1 begins with a value of approximately 0.8, whereas measurement 2 with a value close to 0. This is due to the fact that the first measurement was started only after the filling of the test cell, while measurement 2 was already running during the filling procedure. It can be seen that until approximately 1 minute after filling the calculated values are slightly higher than the measured ones. Between 1 minute and approximately 25 minutes the calculation is below the measurements. After reaching a maximum concentration at about 15 minutes, the concentrations of measurement 1 decrease to 95% at minute 45 and the concentrations of measurement 2 to 98% at minute 35, respectively, while the calculation approximates the value 1. This decrease may result from a chemical reaction of the nitric oxides with air humidity in the test cell or precipitation of NO_2 at the test cell wall, decreasing the NO_2 concentration in the test gas. Additionally, a long-duration measurement for 13 days was carried out, which exhibits a decrease to approximately 35% of the initial value. This observation means that the shock tunnel experiment should be conducted not later than 15 minutes after seeding the test gas in order to avoid a reduction of the tracer gas and a potential corrosion of the shock tube.

It can be summarized that the chosen mechanism is able to describe the formation of NO_2 observed by the measurements in principle. Serving

as an example, the equilibrium concentrations of NO_2 were calculated using this mechanism after filling the test cell with two different mixtures at 298 K and 1 MPa. Initial NO concentrations of 1320 ppm and 1485 ppm lead to equilibrium NO_2 concentrations of 1142 pm and 1266 ppm, respectively. Calculations with mixture 1 at an increased temperature of 353 K showed an increase of the NO_2 concentration to approximately 1303 ppm (see Table 2).

Table 2: Initial concentrations of NO and calculated equilibrium concentrations of NO_2 in the test cell at 1 MPa used for the comparison of the measurements with the reference data

Mixture	Temperature [K]	X_{NO} initial [ppm]	X_{NO2} equ. [ppm]
Mixture 1	298	1320	1142
Mixture 2	298	1485	1266
Mixture 1	353	1320	1303

VI. CONCLUSION

Laser-induced grating spectroscopy (LIGS) is a promising technique for single-shot temperature measurements under harsh conditions, e.g. in the nozzle reservoir of the shock tunnel of the Institute for Thermodynamics at the Bundeswehr University Munich. It was shown in former works at this setup that under moderate conditions seeding of the test gas with NO_2 improves the signal-to-noise ratio by the formation of a thermal grating based on absorption. This grating then can be used for temperature measurements with the laser-induced thermal grating spectroscopy (LITGS). As pure NO_2 is toxic and highly corrosive, for the temperature measurements in the nozzle reservoir of the shock tunnel mixtures consisting of NO, N_2 and air were used instead, leading to the formation of the absorbing species NO_2. For a better understanding and an optimization of the seeding process, in this work the formation and the temporal concentration of NO_2 was investigated experimentally and numerically.

An optical setup was built, which is able to carry out laser absorption measurements in the spectral range from 592 nm to 596 nm. The test setup basically consists of a Nd:YAG laser and a dye laser to generate the spectrally tunable beam, energy sensors and a test cell. For the absorption measurements, the test cell was filled with NO-N_2 test gas and air leading to the formation of NO_2. The comparison of the measured spectral absorption with NO_2 absorption cross sections from reference data showed a good agreement providing the evidence of the NO_2 formation.

Additionally, a reaction mechanism was chosen and analyzed in order to simulate the reaction kinetics under the prevailing conditions in the test cell with the software code Cosilab. This mechanism was validated on the basis of equilibrium states by a comparison with CEA calculations. For the validation of the simulation of the temporal evolution of NO_2 concentrations in freshly seeded air, an absorption measurement was carried out. By normalization of the measurement data by its maximum concentration, normalized concentrations of the absorbing species were calculated. The comparison of this data with Cosilab simulations showed that the selected reaction mechanism is able to predict the increase of the NO_2 concentration after filling the test cell with NO-N_2 test gas and air in principle. In contrast to the calculated values, the measured values decrease after reaching a maximum concentration at 15 minutes. In a long-duration measurement for 13 days, a decrease to 35% of the initial value could be observed. It is assumed that this is either due to chemical reaction of NO_2 with humidity or precipitation of NO_2 at the test cell wall. However, the final reason for this reduction of NO_2 concentration could not be identified during this work.

Summing up, with the presented work it could successfully be demonstrated that seeding with a mixture of NO/N_2 and air leads to a stable formation of NO_2 as tracer species under the conditions investigated. Besides for single-shot temperature measurements in a shock tunnel with LITGS, this comparatively safe and simple seeding technique can be used for any (optical) measurement method based on NO_2 seeding.

REFERENCES

[1]. Schemperg, K., Mundt, Ch., Study of numerical simulations for optimized operation of the free piston shock tunnel HELM, 15th AIAA International Space Planes and Hypersonic Systems and Technologies Conference, AIAA-2008-2653, Dayton, OH, USA, 2008.

[2]. Mundt, Ch., Development of the New Piston-Driven Shock-Tunnel HELM, in: O. Igra, F. Seiler (eds.) Experimental Methods of Shock Wave Research, Volume 9 of the series Shock Wave Science and Technology Reference Library pp. 265-283, (Springer Verlag, 2015).

[3]. Sander, T., Altenhöfer, P., Mundt, C., Development of Laser-Induced Grating Spectroscopy for Application in Shock Tunnels, Journal of Thermophysics and Heat Transfer, Vol. 28, Issue 1, Jan. 2014, pp. 27-31, doi: 10.2514/1.T4131.

[4]. Williams, B., Edwards, M., Stone, R., Williams, J., Ewart, P., High precision in-cylinder gas thermometry using Laser Induced Gratings: Quantitative measurement of evaporative cooling with gasoline/alcohol

blends in a GDI optical engine, Combustion and Flame, Vol. 161, Issue 1, Jan. 2014, pp. 270-279, doi: 10.1016/j.combustflame.2013.07.018.

[5]. Mizukaki, T., Matsuzawa, T., Application of laser-induced thermal acoustics in air to measurement of shock-induced temperature changes, Shock Waves, Vol. 19, Issue 5, Jul. 2009, pp. 361-369, doi: 10.1007/s00193-009-0218-6.

[6]. Kuehner, J. P., Tessier, F. A., Kisoma, A., Flittner, J. G., McErlean, M. R., Measurements of mean and fluctuating temperature in an underexpanded jet using electrostrictive laser-induced gratings, Experiments in Fluids, Vol. 48, Issue 3, Sept. 2010, pp. 421-430, doi: 10.1007/s00348-009-0746-y.

[7]. Cummings, E. B., Laser-induced thermal acoustics: simple accurate gas measurements, Optics Letters, Vol. 19, No. 17, 1 Sep. 1994, pp. 1361-1363, doi: 10.1364/OL.19.001361.

[8]. Cummings, E. B., Leyva, I. A., Hornung, H. G., Laser-induced thermal acoustics (LITA) signals from finite beams, Applied Optics, Vol. 34, No. 18, 20 Jun. 1995, pp. 3290-3302, doi: 10.1364/AO.34.003290.

[9]. Stampanoni-Panariello, A., Kozlov, D. N., Radi, P. P., Hemmerling, B., Gas phase diagnostics by laser-induced gratings I. theory, Applied Physics B, Vol. 81, Issue 1, 3 Jun. 2005, pp. 101-111, doi: 10.1007/s00340-005-1852-z.

[10]. Stampanoni-Panariello, A., Kozlov, D. N., Radi, P. P., Hemmerling, B., Gas phase diagnostics by laser-induced gratings II. experiments, Applied Physics B, Vol. 81, Issue 1, 3 Jun. 2005, pp. 113-129, doi: 10.1007/s00340-005-1853-y.

[11]. Altenhöfer, P., Sander, T., Mundt, Ch., Preliminary Experiments for Temperature Measurements in Shock Tunnels Using Laser-Induced Electrostrictive Gratings, 17th International Space Planes and Hypersonic Systems and Technologies Conference, AIAA-2011-2211, San Francisco, CA, USA, 2011.

[12]. Sander, T., Altenhöfer, P., Mundt, Ch., Temperature Measurements in a Shock Tube using Laser-Induced Thermal Grating Spectroscopy, Proceedings of the 17th International Conference on the Methods of Aerophysical Research (ICMAR), Vol. 1, Jul. 2014, pp. 178-179, Novosibirsk, Russia.

[13]. Sander, T., Altenhöfer, P., Mundt, Ch., Temperature Measurements in a Shock Tube Using Laser-Induced Grating Spectroscopy, Journal of Thermophysics and Heat Transfer, Vol. 30, Issue 1, Jan. 2016, pp. 62-66, doi: 10.2514/1.T4556.

[14]. Selcan, C., Sander, T., Altenhöfer, P., Koroll, F., Mundt, Ch., Stagnation Temperature Measurements in a Shock-Tunnel Facility Using Laser-Induced Grating Spectroscopy, Journal of Thermophysics and Heat Transfer, Volume 32, Issue 1, pp. 226-236, 2018, doi: 10.2514/1.T5199.

[15]. Altenhöfer, P., Sander, T., Koroll, F., Mundt, Ch., LIGS Measurements in the Nozzle Reservoir of a Free-Piston Shock Tunnel, Shock Waves, 2018, doi: 10.1007/s00193-018-0808-2.

[16]. Cosilab, Combustion Simulation Laboratory, Rotexo Software, Rotexo GmbH & Co. KG, Heintzmannstr. 162, 44801 Bochum, Germany, 2011.

[17]. McBride, B. J., Gordon, S., Computer Program for Calculation of Complex Chemical Equilibrium Compositions and Applications: Part II: User's Manual and Program Description, Report Number NASA RP-1311-P2, 1996, Cleveland, OH, USA.

[18]. Pearse, R. W. B., Gaydon, A. G., The Identification of Molecular Spectra, 4th ed., (Chapman and Hall, London, 1976).

[19]. Hsu, D. K., Monts, D. L., Zare, R. N., Spectral Atlas of Nitrogen Dioxide 5530-6480 Angstrom, (Academic Press, New York, ISBN 0-12-357950-3, 1978).

[20]. Vandaele, A. C., Hermans, C., Simon, P. C., Carleer, M., Colin, R., Fally, S., Mérienne, M. F., Jenouvrier, A., Coquart, B., Measurements of the NO_2 absorption cross-section from 42000 cm^{-1} to 10000 cm^{-1} (238-1000 nm) at 220 K and 294 K, Journal of Quantitative Spectroscopy and Radiative Transfer, Vol. 59, Issue 3-5, May 1998, pp. 171-184, doi: 10.1016/S0022-4073(97)00168-4.

[21]. Schneider, W., Moortgat, G. K., Tyndall, G. S., Burrows, J. P., Absorption cross-sections of NO_2 in the UV and visible region (200 - 700 nm) at 298 K, Journal of Photochemistry and Photobiology A: Chemistry, Vol. 40, Issue 2-3, Nov. 1987, pp. 195-217, doi: 10.1016/1010-6030(87)85001-3.

[22]. Burrows, J. P., Dehn, A., Deters, B., Himmelmann, S., Richter, A., Voigt, S., Orphal, J., Atmospheric remote-sensing reference data from GOME: Part 1. Temperature-dependent absorption cross-sections of NO_2 in the 231-794 nm range, Journal of Quantitative Spectroscopy and Radiative Transfer, Vol. 60, Issue 6, Dec. 1998, pp. 1025-1031, doi: 10.1016/S0022-4073(97)00197-0.

[23]. Volkov, E. N., Konnov, A. A., Gula, M., Holtappels, K., Burluka, A. A., Chemistry of NO_2 decomposition at flame temperatures, Proceedings of the 4th European Combustion Meeting, Combustion Institute, Vienna, Austria, 2009.
[24]. Westley, F., Table of Recommended Rate Constants for Chemical Reactions Occurring in Combustion,' Library of Congress Cataloging in Publication Data, Chemical Kinetics Information Center, Washington, D.C., USA, 1980.
[25]. Goswami, M., Volkov, E. N., Konnov, A. A., Bastiaans, R. J. M., de Goey, L. P. H., Updated Kinetic Mechanism for NO_x Prediction and Hydrogen Combustion, Department of Mechanical Engineering, Technische Universiteit Eindhoven, Eindhoven, Netherlands, 2008.
[26]. Atkinson, R., Baulch, D. L., Cox, R. A., Crowley, J. N., Hampson, R. F., Hynes, R. G., Jenkin, M. E., Rossi, M. J., Troe, J., Evaluated kinetic and photochemical data for atmospheric chemistry: Volume I - gas phase reactions of O_x, HO_x, NO_x and SO_x species, Atmospheric Chemistry and Physics, Vol. 4, No. 6, Sep. 2004, pp. 1461-1738, doi: 10.5194/acp-4-1461-2004.
[27]. Baulch, D. L., Bowman, C. T., Cobos, C. J., Cox, R. A., Just, Th., Kerr, J. A., Pilling, M. J., Stocker, D., Troe, J., Tsang, W., Walker, R. W., Warnatz, J., Evaluated Kinetic Data for Combustion Modeling: Supplement II, Journal of Physical and Chemical Reference Data, Vol. 34, No. 3, Jul. 2005, pp. 757-1397, doi: 10.1063/1.1748524.
[28]. Savitzky, A., Golay, M. J. E., Smoothing and Differentiation of Data by Simplified Least Squares Procedures, Analytical Chemistry, Vol. 36, No. 8, Jul. 1964, pp. 1627-1639, doi: 10.1021/ac60214a047.

T. Sander" Investigation of NO2 Absorption Behaviour around 593 nm for Seeding Purposes" International Journal of Engineering Research and Applications (IJERA), Vol. 09, No.08, 2019, pp. 04-11